Surgical Applications of Milli-Robots. *

Michael B. Cohn† Lara S. Crawford†‡ Jeffrey M. Wendlandt§
S. Shankar Sastry†
University of California, Berkeley 94720

Abstract

Minimally invasive surgical techniques, especially endoscopy and laparoscopy, possess many advantages over conventional methods. These include accelerated patient recovery and reduced rate of complications. However, limitations of current operating instruments create difficulties for the surgeon. In this paper, we present a design for an improved polypectomy snare for the endoscope, several rotary actuator designs for endoscopic tools, and a prototype endo-platform, which provides fine motion control for endoscopic tools. We also present several prototypes of more dextrous laparoscopic tools based on the human hand. Finally, we present a sensory glove designed as a natural and dextrous human interface.

*Research supported by the NIH under grant R03RR06996 and the ARO under grant DAAL03-91-G0191. LSC was partially supported by an ONR graduate fellowship. JMW was partially supported by an NSF graduate fellowship. For more details about this project, see http://robotics.eecs.berkeley.edu/research/medical/ on the World Wide Web.

†Department of Electrical Engineering and Computer Sciences
‡Graduate Group in Biophysics
§Department of Mechanical Engineering

List of Figures

List of Tables

1 Introduction

Minimally invasive techniques, including endoscopic (gastrointestinal) and laparoscopic (abdominal) procedures, are revolutionizing the field of surgery. These techniques employ surgical instruments which are inserted into the body through a pre-existing orifice or a small puncture rather than the larger traditional incision. Minimally invasive procedures have several advantages over traditional surgery, the chief being minimization of trauma to healthy tissue. As a result, recovery is accelerated and the risk of complications from infection and scar adhesion is reduced. These considerations have motivated the application of minimally invasive alternatives wherever feasible. However, there are limitations to the operating instruments now used in these procedures which exact a price in surgical access, dexterity, efficiency, and in some cases safety. It is our goal to design improved instruments and human interfaces for endoscopy and laparoscopy. We further envision a teleoperative surgical system which would combine the improved interface and tools for laparoscopy to enhance the surgeon's control of the operation.

2 Minimally-Invasive Surgery

Nearly all minimally invasive procedures employ means for imaging the surgical site in real time. These may be non-invasive, as with fluoroscopy, or invasive, using, for example, an optical fiberscope. Such instruments, or "scopes," may be flexible, like endoscopes, which are employed in the gastrointestinal tract. Modern endoscopes deliver images via a miniature video camera (CCD) at the instrument tip. When the operative site is sufficiently accessible, a rigid scope may be used. The laparoscope, used in abdominal surgery, is a typical example. In this case, the image is focused by lenses in a rigid tube onto an eyepiece at the base of the scope, to which a camera is usually attached. In both endoscopy and laparoscopy, viewing light is delivered to the operative site by fiber optics, and the surgeon views the site on an external CRT. There are several problems inherent in these methods of imaging as compared to direct viewing, including loss of depth perception with the two-dimensional view of the operative field, reduced angle of view, reduced resolution, and lack of ability to pan quickly through the scene ([1]; [2], p. 39, p. 85). Technology such as stereo scopes, which provide a three-dimensional image, is being developed to address these problems; we, however, will focus mainly on instruments and mechanical human interfaces for surgery.

2.1 Endoscopy

Extensive discussion of endoscopic techniques is found in Baillie [3], Siegel [4], and Silverstein and Tytgat [5]. The main piece of equipment is the endoscope, a flexible tube ranging in length from 70–180 cm., typically 11 mm in diameter. Video image controls, air/water/suction controls, position controls, an insertion channel for the tools, and connections to the light source are attached to the end of the scope which is held by the surgeon. The distal end contains a lens to focus an image onto the video chip, the output aperture for the light source, the tool port, and the water/air ports. The left/right, up/down position of the end of the endoscope is controlled by deforming the last 10 cm. of the flexible tube in an

arc using two dials on the outer end of the scope. Surgery in the colon or in the esophagus is performed by inserting various tools through the endoscope to the operation site. The typical diameter of the tool channel is 2.8 mm. Biopsy forceps, polypectomy snares, three-pronged graspers, and cytology brushes (which resemble pipe cleaners) are some of the tools used in endoscopic procedures. The tools used in endoscopy generally possess 1 internal degree of freedom and can be slid in and out of the endoscope. The direction of the tool axis is determined by the viewing direction of the end of the endoscope.

The major limitations in endoscopy are the lack of dexterity in the tools and the lack of fine motion control. For example, biopsies in the esophagus are difficult since the esophageal channel is long and rigid and the biopsies must be performed at right angles to the tool channel. The surgeon must move the entire last 10 cm. of the endoscope to slightly reposition the tool, which is not only too large a scale for some tasks, but also moves the surrounding tissue, further complicating the task. Also, the twist angle about the tool axis is not controllable in current instruments since the tools are long and not torsionally stiff. In this paper, we present a design for a snare-forceps combination to provide greater control when removing polyps from the colon. We also discuss several designs for providing endoscopic tools with rotational control. Additionally, we present a prototype of the endo-platform, a modification of the endoscope which provides fine motion control of the tool.

2.2 Laparoscopy

Discussion of laparoscopic techniques can be found in Graber, *et al.* [2], Semm [6], and Saleh [7]. Laparoscopic surgery takes place in an approximately 20 x 20 x 20 cm. workspace inside the patient created by pumping gas into the abdominal cavity. The laparoscope and laparoscopic instruments enter the body via 5 - 12 mm. diameter cannulae inserted through puncture incisions in the abdominal wall. There are many instruments available for use in laparoscopic procedures, including biopsy forceps, various types of graspers, scissors, electrocautery devices, staplers, needle holders, and suture loops for ligation. Instruments have four degrees of freedom in addition to their internal freedoms (for example, opening and closing a grasper). Most of the instruments' internal freedoms are operated via sliding linkages. The rigidity of the laparoscopic instruments and the use of multiple abdominal sites gives the surgeon more degrees of freedom with which to work than in endoscopic techniques.

There are several limitations of the laparoscopic instruments which make laparoscopy more awkward for the surgeon than traditional "open" surgery. For example, the fixed access point to the abdomen makes it impossible for instruments to reach all positions and orientations. Since the instruments are rigid and unarticulated, they cannot bend around obstacles, making some areas of the abdominal cavity difficult to reach from a given entry point. Also, since the instruments pivot about a fulcrum in the patient's abdominal wall, the instrument tip moves left when the surgeon moves the handle right, and forward when the surgeon moves it back. This type of control likely interferes with a number of reflexes involved in fine manipulation. The lack of dexterity when operating with these instruments makes some tasks, like suturing and knot-tying inside the body cavity, especially difficult ([2], pp. 23–25; [6], p. 98). In addition, the instruments are single-purpose. In order to change from grasping to cutting, for example, one must switch from one instrument to another. In this paper, we present several prototype laparoscopic instruments designed for improved

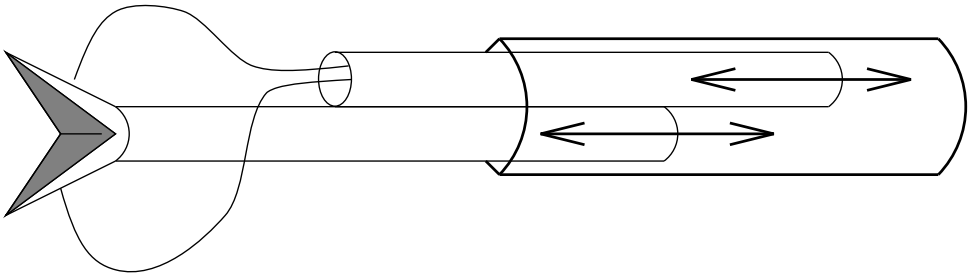

Figure 1: Snare and forceps combination.

dexterity and versatility. We also discuss a prototype glove designed as human interface to these instruments.

3 Endoscopic Manipulators

3.1 Designs

This section describes several designs to provide additional dexterity and control in endoscopic instruments. We also present a prototype of one of the designs and experiments performed on this prototype.

Currently, polyps are severed by positioning a polypectomy snare over the polyp and tightening it as cautery current is applied. The polyp is then removed through the scope's suction channel. This process might be simplified with a combination of the snare and a biopsy forceps in which the forceps is positioned inside the snare opening (See Figure 1). The snare and forceps can move in and out relative to each other. With this device, the biopsy forceps can grasp the polyp and hold it while the snare is moved over the polyp and tightened. This is easier than trying to maneuver the snare around the polyp without the forceps to hold it steady. The forceps can then keep the polyp away from the wall of the colon while cauterization is applied through the snare, so the current is concentrated at the base of the polyp and cannot diffuse out of the polyp through contact with the colon walls. The severed polyp can be retrieved by simply bringing it into the instrument/suction channel with the forceps.

We have several concept designs to provide rotary motion about the tool's axis, although none have been prototyped at this time. The first design uses a high pitch screw in a fixed housing attached to a small piston such as those described in [8]; see Figure 2. As the piston pushes or pulls the screw through the housing, the tool rotates. The bellows seal the tool channel and permits its expansion. The housing of the tool needs to be secured to the operating part of the tool. In current snares, for example, the housing is a plastic tube which is not fixed to the wire snare, but can be made to be rotationally fixed through design modifications.

The second design for rotational motion is composed of a central pulley and two smaller pulleys driven by tendons. The central pulley is secured to the tool. As the tendons are pulled, the central pulley spins in the fixed housing, rotating the tool. This design is shown in Figure 3.

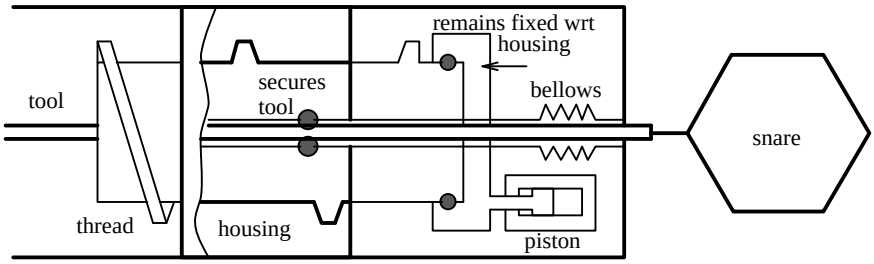

Figure 2: Rotary screw actuator.

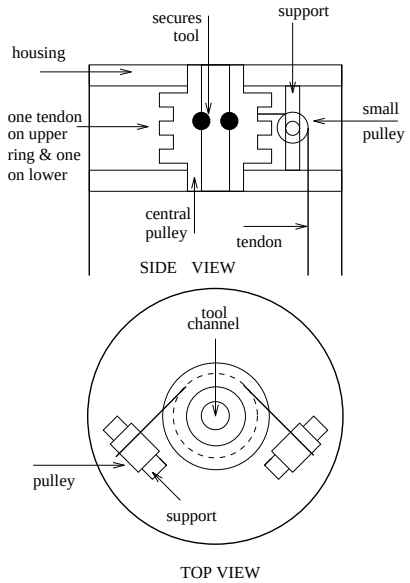

Figure 3: Rotary pulley actuator.

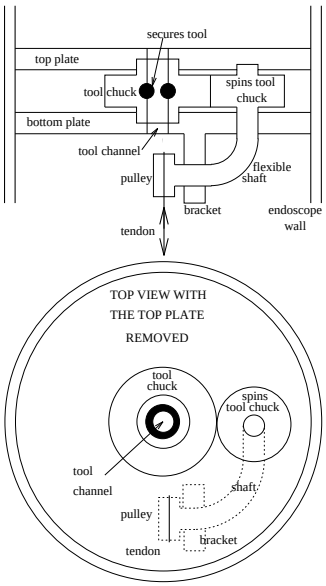

Figure 4: Flexible rotary-shaft actuator.

The third design, shown in Figure 4, uses a flexible shaft to transform linear motion along an axis to rotation about the same axis. The tool is secured in a central tool chuck with an O-ring. Pulling the tendons rotates a pulley attached to the flexible shaft, which causes the shaft to rotate as well. The shaft bends through ninety degrees and transmits its rotation to a cylinder attached to its other end. This cylinder spins the chuck, causing the tool to rotate.

As mentioned above, the surgeon can only reposition the tool by bending the last 10 cm. of the endoscope or by sliding the tool in and out of the tool channel. Sometimes the tool can also be repositioned by moving the patient and pushing on the patient's abdomen. We have designed a device, the endo-platform (see Figure 5), which allows more precise tool positioning and will allow the surgeon to reorient the tool without moving the surrounding tissue. The platform is composed of two plates separated by a rigid tube and a short spring, through which the tool passes. The diameter of the plates is the same as that of the endoscope. The spring serves as a spherical joint which resists side forces and provides a pivot point. Three tendons running between the plates can be pulled individually to change the orientation of the outer plate relative to the inner plate and move the tool tip. Any linear actuators that meet the force and space requirements can be substituted for the tendons, however. The lens and the CCD array are attached to the outer plate so that the view field moves along with the tool. The water channels are extended flexibly between the plates to accommodate the motion. The entire assembly is designed to be attached to the end of an existing endoscope. Large motions can be controlled as before by deforming the last 10 cm. of the scope, while fine motions are accomplished by reorienting the outer plate of the endo-platform.

We plan to use a joystick as the user interface for the endo-platform. The joystick will be located at the base of the tool channel, and the tool will be inserted through its center. The endo-platform can also be combined with one of the rotary actuators described above

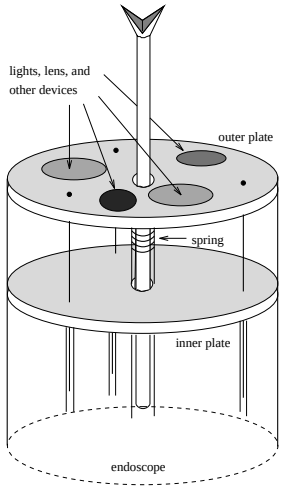

Figure 5: Endo-platform.

to further increase the tool's dexterity. The rotary actuator can then be controlled by a dial attached to the tip of the joystick which rotates about the joystick axis.

3.2 Prototype

We have constructed a prototype of the endo-platform (see Figures 6 and 7) and have demonstrated the device's ability to

position endoscopic tools. The diameter of the plates is 19 mm. (but could easily be scaled to 11mm.), and the length of the device is less than 20 mm. from plate to plate. The three tendons are attached to pulleys on DC servomotors with optical position encoders. The endo-platform is capable of 90 degree deflection in any direction. The kinematics and dynamics of the device and a simulation of a closed-loop controller are described in detail in [9] and [10]. We have implemented a closed loop controller with an update rate of 500 Hz to position the endoscopic tools; our experimental results are described below.

Initially, we used 0.16 mm. stainless steel tendons, which resist tensile forces up to 12 Newtons (N). With the tool at a 45 degree angle and a single motor pulling at 1.7 N, a 0.6 N force was produced at the tool tip 11 mm. from the end of the endo-platform. Thus, at the tensile strength of the metal tendons, a 4.2 N force could be produced. We are currently using Kevlar tendons since 0.1 mm. Kevlar tendons have a tensile strength of 37 N and are more durable than the metal tendons. At the tensile strength of the Kevlar tendons, a 13 N force is produced at the tool tip.

To test the dynamic response of the controlled endo-platform, we commanded the tool to point at an approximately 40 degree angle from the home configuration and recorded the position response. The position response of the tool coordinates is shown in Figure 8. The tool coordinates specify the pointing direction of the tool in terms of modified stereographic projection coordinates. The final pointing angle is approximately 39 degrees. The solid lines

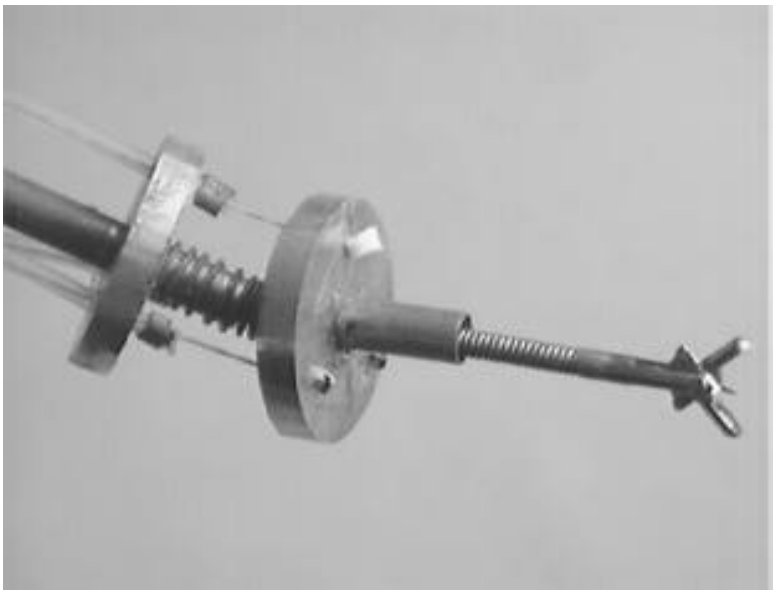

Figure 6: Endo-platform positioning biopsy forceps.

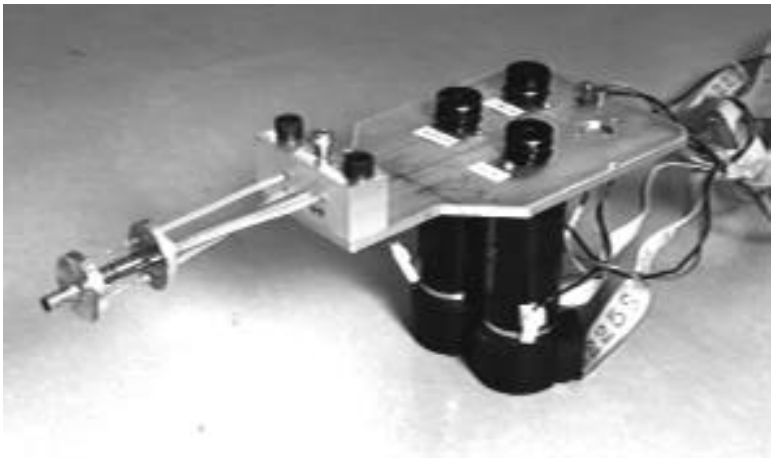

Figure 7: Endo-platform and the tendon drivers.

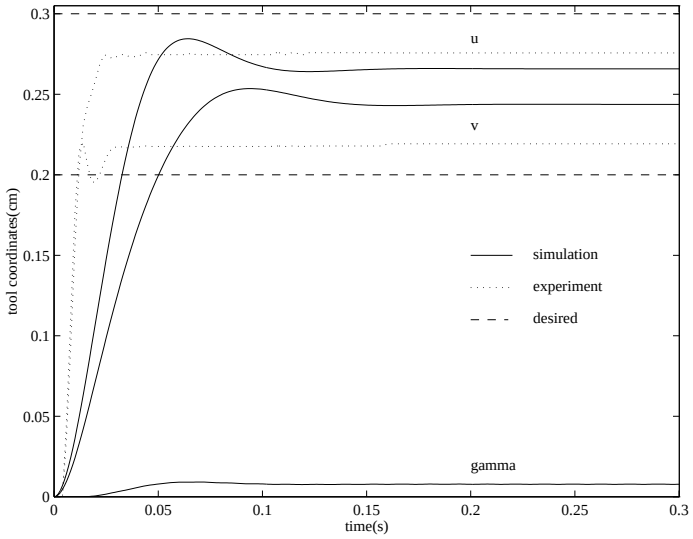

Figure 8: Controlled Step Response

in Figure 8 are the simulation results, the dashed lines are the desired positions and the dotted lines are the experimental results. The bottom graph is the amount of twist around the tool axis as predicted by the simulation. The controller used in the simulation and the experimental controller differ slightly, and the experimental controller leads to a faster response in tool positioning.

The second dynamic test involved tracking a circle at 2.0 Hz (traversing the circle 2 times a second). The desired circle has a radius of 0.3 cm. in the tool coordinates which corresponds to a pointing angle of approximately 33 degrees. The result of this test is seen in Figure 9 where the desired circle, the simulated response, and the experimental response of the endo-platform are shown. We conjecture that the experimental response does not reach the outer edge of the desired circle in the lower left quadrant because the spring force is not radially symmetric. Planned design improvements of the endo-platform should remove this effect. The current prototype is also capable of tracking circles at higher frequencies. We are able to track circles at 20.0 Hz with roughly the same radius as in the 2.0 Hz case. For the 2.0 Hz circle, the radius fluctuates between 0.21 cm. and 0.31 cm. For a 10 Hz circle, the radius fluctuates between 0.12 cm. and 0.26 cm. At 20 Hz, the fluctuation is between 0.11 cm. and 0.27 cm. Increasing the frequency to 30 Hz results in the radius fluctuating between 0.03 cm. and 0.19 cm. At 100 Hz, the radius is essentially zero. Further work needs to be done to improve the system's performance, reliability, and repeatability.

In the future, we plan on modifying the mechanical design of our first prototype to improve the ability to track trajectories and to position endoscopic tools efficiently and reliably. We also plan on improving the control algorithm to improve its accuracy and reliability. Our first prototype has been instructive in the control and design of future endo-platforms.

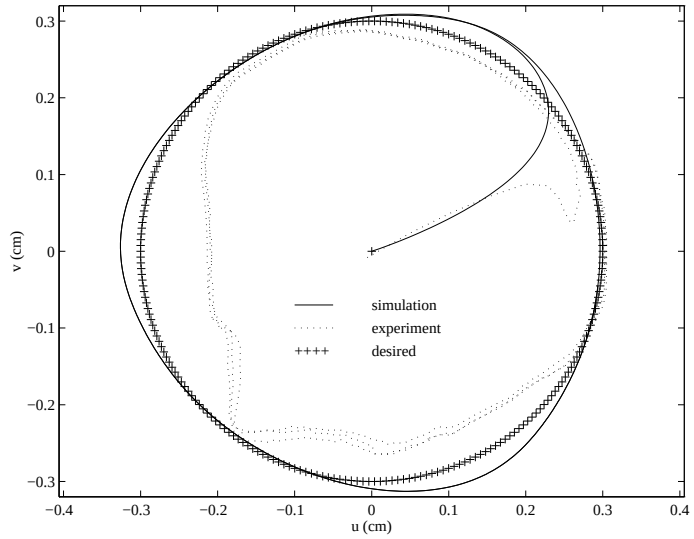

Figure 9: Tracking a Circle at 2.0 Hz

4 Laparoscopic Manipulators

4.1 Design Goals and Prototypes

As mentioned, there are several limitations to current laparoscopic manipulators, and any attempt to address these must meet certain engineering constraints. Devices in current use are able to pass through a 5 - 12 mm. diameter cannula; general-purpose graspers and needle-holders are able to transmit forces of approximately 10 N in any direction, based on force measurements in generic grasping tasks. In addition, in a new instrument, a peak velocity of 20 cm/s would be desirable, based on an estimate of human hand velocities in similar tasks. Finally, a frequency response of 10 - 20 Hz is a useful minimum, based on the range of human hand bandwidth (see section 5.1 below). We have focused on the problem of suturing, as well as the need for a more versatile tool to replace the single-purpose devices which have evolved for specific surgical tasks. We have proceeded under the assumption that significant advances would call for new actuator technology to meet both size and cost constraints.

Initially, we envisioned a many-degree-of-freedom end-effector (robot hand) as a laparoscopic instrument. Such an instrument, based on the human hand, would allow extremely dextrous manipulation. One question was whether any practical improvement over the available one- or two-axis instruments was feasible, given the need to assemble the numerous small parts that would compose a millimeter-scale manipulator. As a result, we directed our efforts toward integrated fabrication approaches characteristic of the IC manufacturing process. Such an approach would potentially eliminate most of the assembly steps.

Our first-cut design was for a roughly anthropomorphic hand fitting in a 10 mm. diameter, 25 mm. long cylinder. Each finger was comprised of an elongated balloon, ribbed to allow expansion only on the dorsal surface and in a longitudinal direction (see Figure 10). In this way, inflating the finger with air caused it to curl. The design was inspired by the flexible

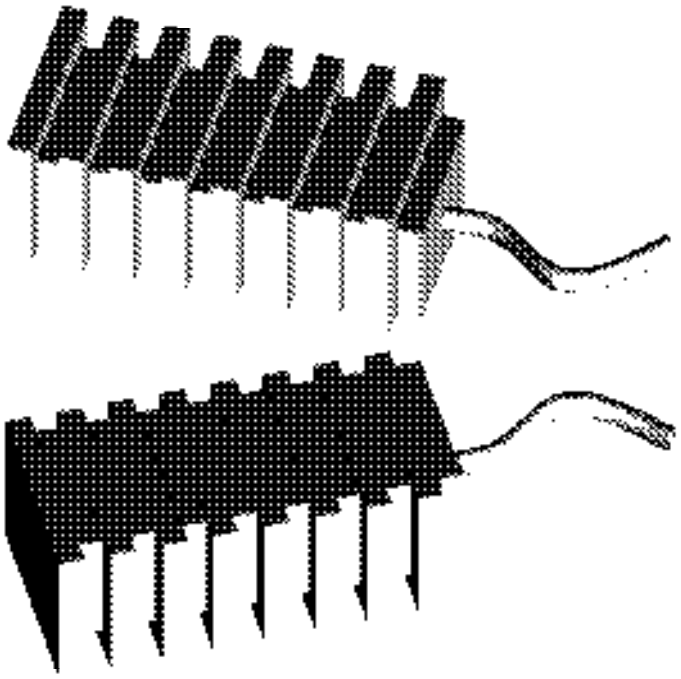

Figure 10: Laparoscopic manipulator fingers, constructed as molded rubber balloons.

micro-actuator of Suzumori [11]. The fingers were built up in layers of molded silicone rubber (Dupont 3112 RTV). The molds were created in machinable wax, using a table-top CNC (computer numerically controlled) mill (Spectralight mill, Light Machines Corp., Nashua, NH). With this technique, we could attain 50 μ accuracy and 500 μ line width.

The main problems with the anthropomorphic hand were its low force output and poor controllability. The force in this configuration is proportional to the operating pressure, the cross-section, and the ratio of finger radius to length; in our prototype,

$$\frac{2 \times 10^5 \text{Pa} \cdot 8\text{mm}^2 \cdot 2\text{mm}}{25\text{mm}} = 0.13\text{N}.$$

This force output was at least an order of magnitude lower than desired, mainly because of the low burst pressure of the unreinforced rubber (2×10^5 Pascals). In addition, while the all-rubber design simplified fabrication and miniaturization, the finger structure was highly compliant and had an effectively infinite number of freedoms. Since there was only one control, the system was underconstrained, which would lead to problems whenever the manipulator encountered significant opposing forces.

In the second prototype, a more robust, controllable device was desired, particularly for the suturing task. We used the molding technique again, but with rigid materials such as polyester and epoxy, to fabricate jointed fingers with a structure similar to that of a bicycle chain. These fingers were approximately 10 mm. long and 2.5 mm. in diameter. We incorporated the fingers into hand-like end-effectors having two fingers and a thumb, as well as a single-axis wrist (see Figure 11). The hands were actuated using 0.1 mm. tendons. A typical example possessed seven degrees of freedom: two in each of three fingers, and one in the wrist.

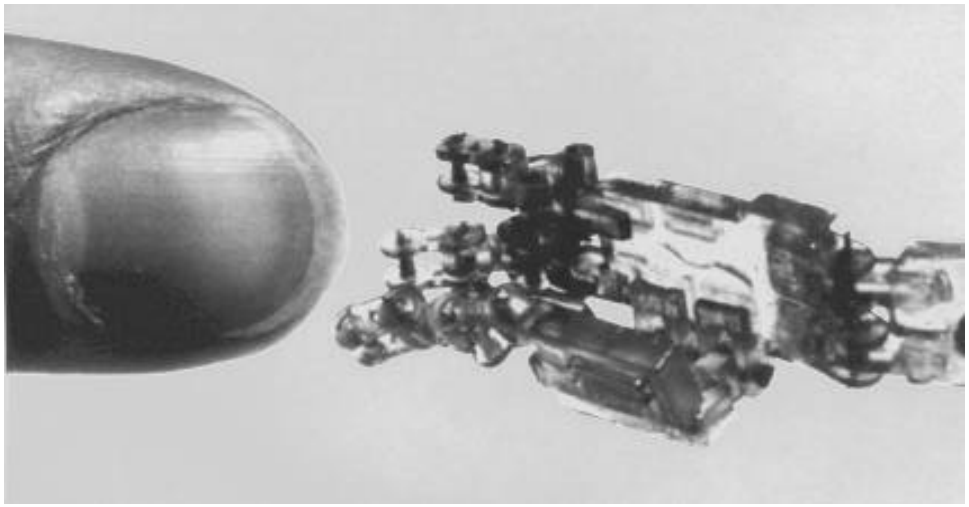

Figure 11: Hand-like end-effector.

This design displayed acceptable dexterity, but had several limitations. Chief among these was insufficient force output (in the range of several hundred milliNewtons). Under larger forces, the casting resin used in the device tended to fracture, though this problem could be reduced by using a more robust resin. The Kevlar tendons had surprising strength, as mentioned above, and therefore should not be a limitation in future designs. Other limitations of this design included the friction and backlash introduced by the joints, the friction due to routing tendons through the hand, and the kinematic problems inherent in tendon-driven serial links [12], as well as potential manufacturing problems. Nevertheless, in the 1 N range, the device displayed surprising capability; under simple marionette-style control, it could grasp and manipulate objects, and the system's frequency response was clearly above the range of the user's hand motions.

In our final design, we addressed the problem of force output by using piston actuators, which combine high force and stiff output in a small package. We also simplified the manipulator design by replacing the multifingered end-effector with a two-jaw gripper, in order to make the device more robust while still enabling it to perform the majority of surgical tasks. In addition, compact actuators and a reduced number of axes opened the possibility of a direct-drive design, i.e. with the actuators placed directly in the end-effector links. This design would simplify both kinematics and mass-production.

Again employing the CNC casting process, we produced several prototype cylinders as well as a two-axis end-effector with a claw-like gripper and a one-axis wrist. (It should be borne in mind that a laparoscopic instrument already has one degree of orientational freedom via rotation about its long axis; a full three degrees of freedom are gained from a two-axis wrist in the body cavity.) The end-effector had a length of 43 mm. (from the wrist joint to the tip of the gripper) and a diameter of 10 mm. (see Figure 12). This manipulator fits well within the anatomical workspace constraints described above, which would dictate that the wrist's center of rotation should be no more than 5 - 10 cm. from the tip of the end-effector. The device demonstrated gripping and tangential forces of 1.9 N and 0.5 N respectively. Subsequent cylinders and two-jaw grippers were fabricated in metal and generated gripping

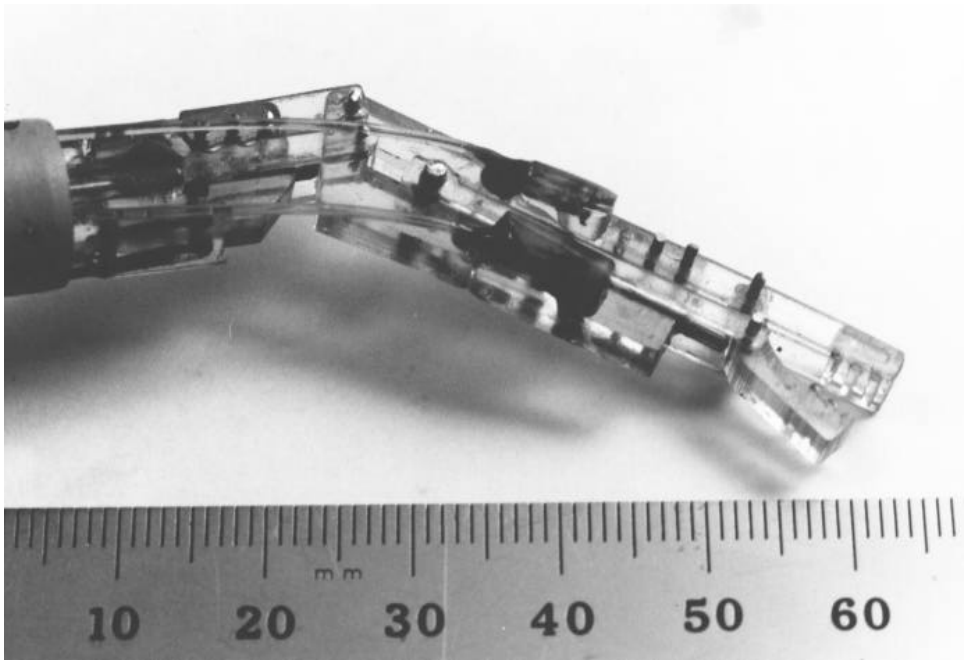

Figure 12: Hydraulic end-effector with two degrees of freedom.

forces in excess of 3 N.

Though there were several initial difficulties with this approach – such as creating reliable connectors – it seems favorable for millimeter-scale surgical manipulators since large forces can be generated. Force output is proportional to operating pressure, and the fundamental limit on this quantity is the tensile strength of the structural materials.

4.2 Future Work

Future work will focus on implementation of a two-axis wrist, as well as position, tactile, and force feedback. Dimensional analysis of the generic piston actuator indicates that a wrist fitting within the 10 mm. diameter constraint could generate adequate torques. Force feedback could assist in suture and knot tensioning as well as guard against inadvertent laceration of tissue outside of the scope's field of view. Tactile sensing might be useful for manipulating suture material or other objects held in the gripper, localizing small anatomical features such as subsurface blood vessels, or detecting features which are obscured from the video camera. We hope to implement tactile feedback using strain sensor arrays on the end-effector coupled to stimulator arrays worn on the surgeon's fingertips. A "teletaction" system has recently been demonstrated [13] and tactile sensors spanning the 1 mm. to 3 cm. size range are being developed in our laboratory. The tactile sensors have a resolution of 64 to 128 elements and employ capacitive sensing [14], [15]. The stimulator is a 25 element (5×5) array of air pistons spanning a 1 cm. square area. This system allows tactile features to be localized with 100 μ accuracy.

One possible ramification of capacitive tactile sensing would be permittivity sensing (the electrostatic equivalent of metal detection). With a simple modification, a capacitive tactile

sensor element could be made insensitive to applied stress, in which case it would respond only to the varying dielectric properties of its environment. Water has a particularly high dielectric constant of about 80, making most tissue easily detectable. Fatty tissue, composed mainly of non-polar molecules, would be have a lower dielectric constant. Blood vessels should be particularly distinguishable, and cancerous tissue, with its increased water content, might be as well. (See [16], [17], [18] for the dielectric properties of tissues and cells.)

5 Human Interface

5.1 Design Issues

In designing the human interface for a teleoperative task, there are many issues to consider, some of which have already been mentioned above. Analyses of these issues can be found in Brooks [19], Brooks and Bejczy [20], Burdea and Zhuang [21], Fischer, Daniel, and Siva [22], McAffee and Fiorini [23], and Sheridan [24]. One of the first questions is whether a non-dextrous controller will suffice for the specific teleoperative system. These devices range in complexity from knobs, joysticks, and teach pendants to universal 6-degree-of-freedom force-reflecting hand controllers (see [23], [20], [25], [22], [26], [27]). For systems with many degrees of freedom or highly anthropomorphic slaves, however, a dextrous master may be required. A dextrous master is an anthropomorphic sensing device worn by the operator to take advantage of the many degrees of freedom (twenty without the wrist [21]) and natural dexterity of the human hand. One commercially available dextrous master that has been popular for teleoperation applications is the VPL DataGlove^{TM}, which uses flexible optical fibers on the back of a glove to sense the amount of bending of the finger joints; the more a joint flexes, the less light is transmitted through the optical fiber (see [28]). The DataGlove measures fourteen degrees of freedom on the hand (see [24], [29], [30]). A second commercially available dextrous master is the Exos Dextrous Hand Master^{TM} (DHM). The DHM is an exoskeleton that attaches to the joints of the hand and uses Hall-effect sensors to measure joint angles. It measures a total of sixteen degrees of freedom ([31], [28], [24], [30]). Another commercially available dextrous master is Virtual Technologies' CyberGlove^{TM}, which uses resistive sensors to measure joint angles. The standard CyberGlove measures eighteen degrees of freedom including wrist pitch and yaw. An augmented version of the CyberGlove measures twenty-two degrees of freedom [32]. All of these masters can be coupled with a Polhemus or other global sensor to give the position and orientation of the whole hand.

One requirement that is often mentioned for a human interface is that it should make a system "transparent," or that it should allow the operator to feel telepresence. There are two issues that strongly influence the transparency of the system: the stimulus-response compatibility of the controller, and the amount and quality of feedback to the controller. Stimulus-response compatibility is a natural correspondence between the movements of the operator and the movements of the manipulator; for example, when an operator moves a joystick left, he or she expects the manipulator to move left as well, in some intuitive frame of reference. For a dextrous master, good stimulus-response compatibility may require complex calibrations to accurately map the operator's joint movements to the manipulator's joint movements and discriminate between different human grasps. Readings from the VPL

DataGlove sensors, for example, do not correspond directly to the joint angles of the hand and may be extensively correlated with each other (see [29]; [30]; [24]).

Force feedback enhances telepresence by presenting information about the magnitude of contact forces in a natural way, while tactile feedback presents information about texture and vibration. The importance of force feedback has been stressed by many authors ([33], [25], [21], [34], [24]), and studies have shown that teleoperative tasks are completed faster or more accurately when the operator has force feedback available ([35], [36], [37], [24], [34]). Although there are many non-dextrous controllers available with force feedback, and have been for many years (see [20], [35], [36], [23], [25], [34], [24]) dextrous controllers with force feedback are still an area of ongoing research. None of the commercially available dextrous masters of which we are aware has force feedback. Various prototypes exist, however, and several are discussed by Burdea and Zhuang in [38]. Tactile feedback is even less developed; tactile sensing and display systems are currently bulky and difficult to implement (see [13], [14], [37]). Other factors influencing the feel of a teleoperative interface are the impedance, loop gains, and informational bandwidth of the master-slave system. A discussion of the human-machine impedance and factors affecting the perceived force feedback can be found in Burdea and Zhuang ([21]). Discussions of impedance, damping, and inertia in teleoperative systems can be found in [21], [24], and [22]. Fischer, *et al.* [22], also address gain ratios and velocity, acceleration, and force maxima. According to Brooks ([19]), the human hand can output information at a maximum rate of 5–10 Hz (1–2 Hz for unexpected signals, 2–5 Hz for periodic signals, about 5 Hz for "internally generated or learned trajectories," and about 10 Hz for reflexes). It can receive information at 20 to 30 Hz for force (kinesthetic) and position feedback and up to about 320 Hz for tactile feedback. Different authors have differing views on what bandwidth is needed for teleoperation, however (see [34], [22], e.g.). Brooks' survey of teleoperator experts obtained a minimum required bandwidth of 3.9 Hz and preferred bandwidth of 9.7 Hz ([19]).

Finally, the operator's safety, comfort, fatigue level, and ability to use the controller with a single hand, as well as the cost of the device, are all important issues in designing a human interface.

5.2 Prototype

For the endo-platform device, a simple, nondextrous master such as a joystick is sufficient for natural control. The laparoscopic manipulator, however, is more complex and may require a more complex, dextrous human interface. The commercially available dextrous masters are not ideal because they are quite expensive and have many more degrees of freedom than we need for controlling the prototype robotic hand. Based on the considerations above, we have designed and built a prototype human interface for the laparoscopic telesurgical system. We decided on a glove-like dextrous master. For a telesurgical application, this kind of anthropomorphic dextrous controller is particularly appropriate, since the surgeon has a high degree of manual dexterity and is experienced with hand-held tools. The glove-like device will also have good stimulus-response compatibility with an articulated robot hand. The current human interface in laparoscopy lacks this compatibility, as mentioned in section 2.2. The prototype glove does not incorporate force feedback at this time.

The glove senses thumb and index finger flexion, wrist flexion, and wrist rotation. It thus

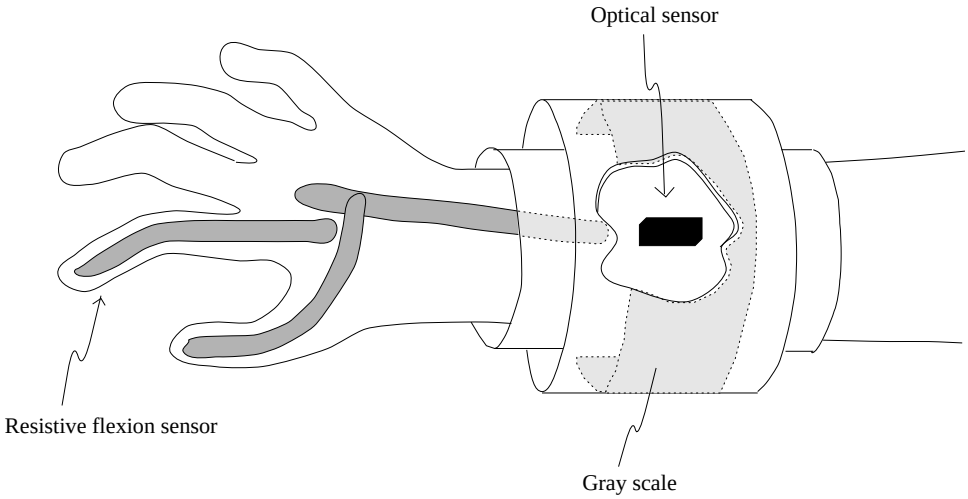

Figure 13: Schematic diagram of glove design.

has sufficient degrees of freedom to control the miniature robotic hand prototype, which has a flexible wrist and a simple gripper (as discussed above). The flexion sensors are constructed using resistive strips from a Nintendo Power Glove^{TM} which change resistance when bent. The useful range of motion is approximately 120 degrees, and the active length of the sensor is approximately 10 cm. Three strips are attached to a lycra glove on the dorsal side of the hand. In our current setup, these sensors have a resolution on the order of 3 degrees for repeated bending at one point. The wrist rotation sensor is made from two concentric plastic tubes (see Figures 13 and 14).

The inner tube has a reflective-mode photosensor mounted in it, and the outer tube has a grayscale attached to its inner surface. When the two cylinders are rotated with respect to one another, the photosensor moves along the grayscale. The inner tube is hinged to allow the operator to insert his or her wrist, and is secured to the operator's wrist with a velcro strip. The inner tube then fits snugly inside the outer tube.

5.3 Rotation Sensor Data

The grayscale producing the most linear data was generated by a logarithmic function with a small polynomial component added. The scale was printed on a 400 dpi laser printer. We tested the linearity by sampling the sensor output every .5 inches along the circumference of the outer tube (about every 16.2 degrees). Four data sets were taken in this manner, in different conditions designed to test the resolution and repeatability of the device. The best linear fit had a slope of 1.94 volts per radian over a range of about 3.4 radians. On average, the error at each data point was 1.5% of the linear fit value. Flaws in the grayscale can cause irregularities in the sensor output; printing the grayscale on a higher quality printer would probably improve the sensor's performance. Also, the output slope can change slightly each time the apparatus is assembled, so the rotation sensor needs to be calibrated each time it is used. The sensor output can then be mapped directly to the rotation of the robotic hand about its axis.

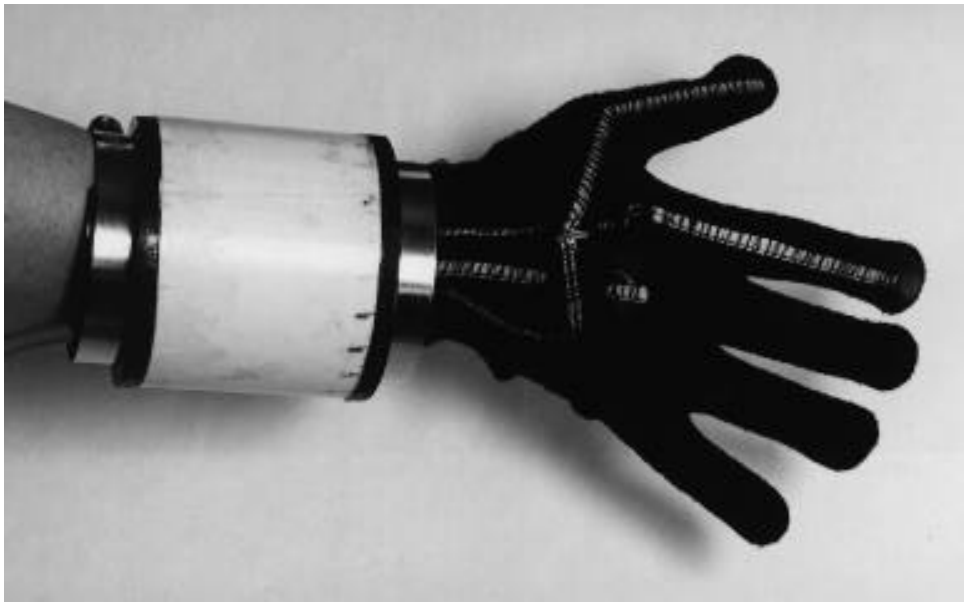

Figure 14: Prototype glove device.

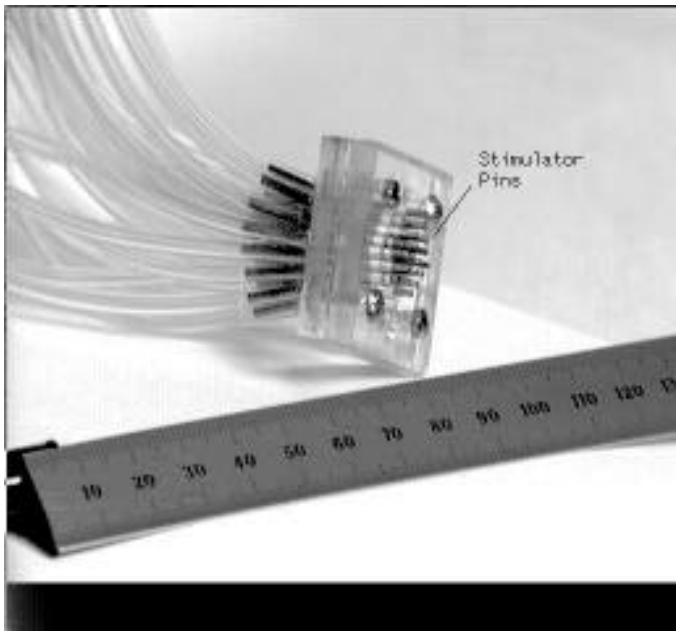

Figure 15: Finger-wearable tactile display constructed in the UC Berkeley Robotics Laboratory.

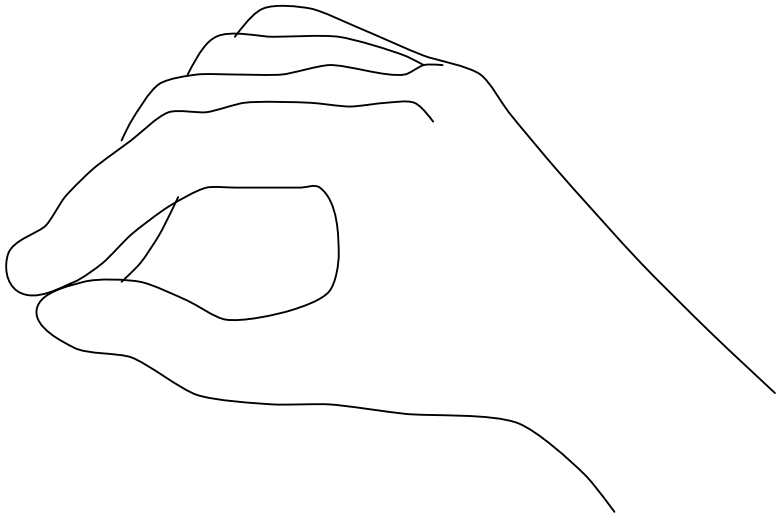

Figure 16: Diagram of pincing position used in calibration and movement tests.

5.4 Flex Sensor Data

In order to map the bend sensor readings to appropriate output signals for the miniature robotic hand, the glove device needs to be calibrated. There are two issues involved: determining how the joint angles of the human hand map to sensor readings, and determining how the hand angles should map to the joint angles of the robot (see [29] and [30] for approaches to the first and second issues, respectively). In our system there is considerable degeneracy in both of these mappings, since there is only one bend sensor each for the index finger and thumb (so the glove really measures overall curvature of these fingers, not joint angles) and the robot has only a one-degree-of-freedom wrist and a gripper. The sensor readings can be functionally mapped to the robotic joint positions, however, by mapping the sensor readings taken from standard hand poses to similar standard poses of the robotic hand. Each operator will have a slightly different map.

We have concentrated on the grasps the surgeon uses for suturing. Since the master device is designed to control a robotic hand that can grasp a needle directly, we used the grasp a surgeon employs with a hand-held needle (rather than a needle-holder) for the calibration procedure. This needle is grasped with the thumb on one side and the index and middle fingers on the other ([39], pp. 58–60; see Figure 16). This thumb-two finger grasp permits precise, dextrous manipulation. The pincing grip of the thumb and fingers corresponds to the gripper action of the current robotic prototype.

We developed a simple calibration procedure to take sensor readings from four right-handed subjects' hands in nine standard poses. The poses were relaxed hand position, wrist held flat, wrist maximally flexed (downward), maximally open hand position (index finger and thumb spread as far as possible), and pincing position (the thumb-two finger grasp). Each subject went through this calibration procedure twice, once before and once after tests designed to assess the consistency and relevance of the calibration measurements. For the first of these tests, subjects were asked to move their wrists smoothly up and down, with the peaks and valleys of the movement synchronized with a timer. Then, for the second test, they were instructed to move smoothly between a comfortable open position and the pincing

Calibration Data for Prototype Glove Device

subject	relaxed wrist (36)	flat wrist (6)	flexed wrist (6)	relaxed index (36)	open index (6)	pinced index (18)	relaxed thumb (36)	open thumb (6)	pinced thumb (18)
DB	5.254	5.126	6.622	5.829	5.657	7.323	5.954	6.114	6.669
	0.109	0.064	0.322	0.211	0.022	0.211	0.105	0.045	0.246
AC	6.091*	5.145	7.063	5.882*	5.642	7.028	5.997*	6.199	6.333
	0.129*	0.016	0.129	0.282*	0.027	0.177	0.129*	0.209	0.122
LC	5.461	5.061	6.882	5.844	5.676	7.457	5.952	5.943	6.694
	0.190	0.031	0.209	0.206	0.046	0.105	0.064	0.144	0.076
DM	6.065	5.213	7.370	5.728	5.674	7.275	5.955	6.272	6.318
	0.141	0.067	0.034	0.063	0.055	0.144	0.067	0.043	0.160

Table 1: Mean and standard deviation of calibration values for all subjects, in volts. Numbers in parentheses indicate total number of samples (both calibration runs combined). Top figure is mean, bottom is standard deviation for each subject. *Only 35 values were recorded for the relaxed position for subject AC.

position, again with the endpoints of the movement coinciding with the timer beeps. The sensor readings for each test were recorded every tenth of a second for ten to eleven seconds, and then the tests were repeated.

The mean and standard deviation of the calibration values for all four subjects are shown in Table 1. Although there are differences between subjects, the pattern of relationships among calibration values is fairly consistent across subjects. The timed movement data from subject DM (a fairly typical data set) is shown in Figure 17. In these plots, the average calibration values for this subject are shown as horizontal lines. More detailed calibration data, movement data from all four subjects, and discussion of the calibration procedure and data can be found in [40].

For the stylized movements tested, the calibration values appear to be fairly consistent with the values recorded during movement for both the index finger and the wrist. The thumb movement traces have smaller amplitudes and much more variation than those of the index and wrist, even within a single trial, and do not correspond well with the thumb calibration values. Unfortunately, since the sensors do not detect individual joint angles, a pincing position in which the thumb and fingers are more rounded and make contact on their tips will give a higher sensor reading than one in which they make contact on the pads. A subject might adopt a slightly different pincing pose for each cycle, which could be causing the thumb variability. For the current prototype, we decided to use the more consistent index reading to control the robot gripper position. For the index, we can plausibly map

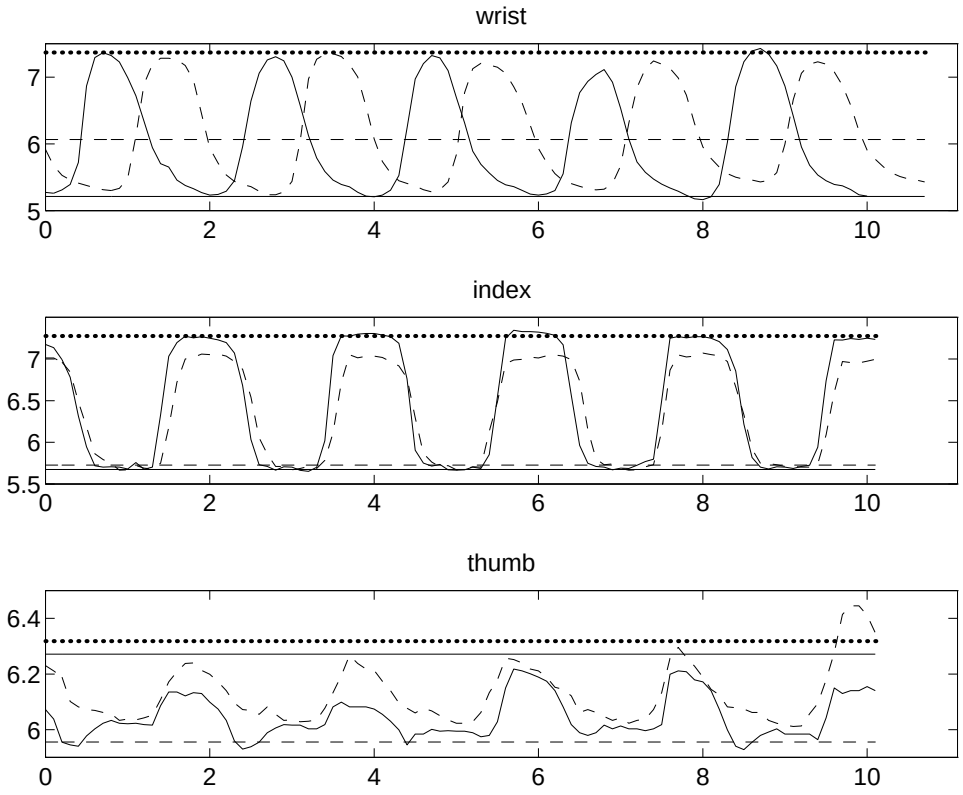

Figure 17: Movement data for subject DM (first trial is solid trace, second trial is dashed trace). Calibration data averages are shown as horizontal lines. For wrist: flat=solid, relaxed=dashed, flexed=dotted. For index and thumb: open=solid, relaxed=dashed, pincing=dotted. Horizontal axis is seconds and vertical axis is volts for each plot.

the open calibration value (and anything below it) to a fully open gripper and the pincing value (and anything above it) to a fully closed gripper. The intermediate values correspond to intermediate states of the gripper. A similar map can be used for the wrist. The subjects were instructed not to bend their wrists upward past the flat position, since the wrist flex sensor tended to buckle when the wrist was bent upward, producing anomalous readings.

5.5 Future Work

The prototype glove has several advantages for use in telesurgery. It is simply constructed, it incorporates wrist rotation and flexion sensors, and it is lightweight and non-fatiguing. It makes use of the natural correspondence between thumb and index finger pincing and the robot's gripper action. Since the sensor signals can be mapped directly to desired positions of the robot joints, very little computation is needed for position control of the slave, and the preliminary data suggests that the glove will function well as a master for test suturing tasks. Many improvements can be made on this initial prototype, however. To more accurately sense finger, and especially thumb, position, the glove should have separate flex sensors for each joint. The glove should also incorporate a sensor to measure upward wrist flexion as well as downward. Future prototypes should have an improved physical design to ease putting on and removing the glove. The main drawback of this glove prototype, and indeed any glove, is the difficulty of incorporating force feedback. The lack of force feedback in the prototype has proven to be a disadvantage in test teleoperative tasks. The lack of a suitable actuator technology, however, makes incorporating force feedback into a glove difficult. In the future, we may sacrifice some dexterity by switching to a master device based on a more conventional design, such as a Stewart platform, in order to make use of force feedback. Tactile feedback will be incorporated into future masters as well.

6 Telesurgical Workstation

As a step toward a teleoperative surgical workstation (see Figures 18 and 19), we have installed the prototype robotic

manipulator and glove on a robotic platform. The platform can provide the manipulator with x, y, and z (vertical) positioning and rotation (θ) about the z axis and can sense force in the z and θ axes. The x, y, z, and θ control signals may be generated by a sensor attached to the glove or by simply using a second module of the platform as a master for the global position. The wrist and gripper of the manipulator are controlled by the wrist and finger readings of the glove, as described above. Preliminary open-loop tests (run at 10 Hz) of the gripper and wrist controls have been promising. The glove has also been tested in simple teleoperative tasks (picking up a small object) with larger fingers equipped with tactile sensors that were developed in our laboratory (see [41]). The tactile display, mounted on the first finger of the glove, rendered the force image obtained by the tactile sensors, providing detailed grip force and object position information in real-time. The platform will help to evaluate prototypes' effectiveness in laparoscopic tasks such as suturing, and will help identify problems in designing a teleoperative workstation for use in the operating room. The main hurdles we foresee include making the platform compact enough and simple

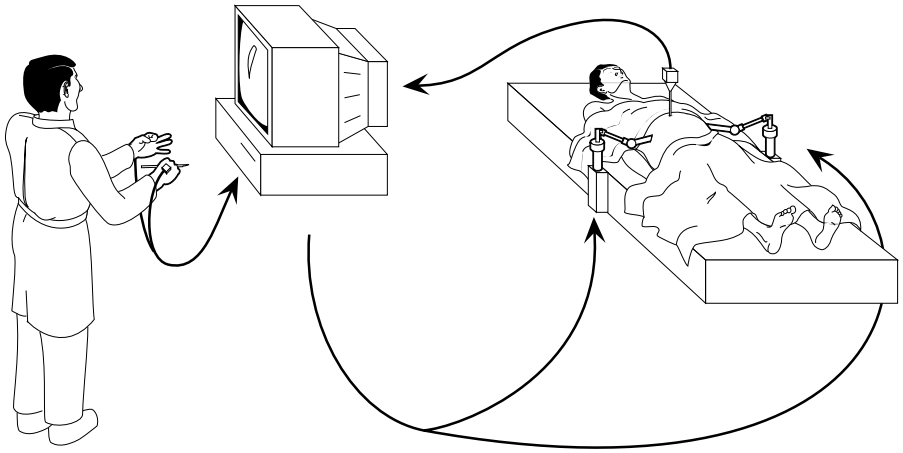

Figure 18: Telesurgical workstation.

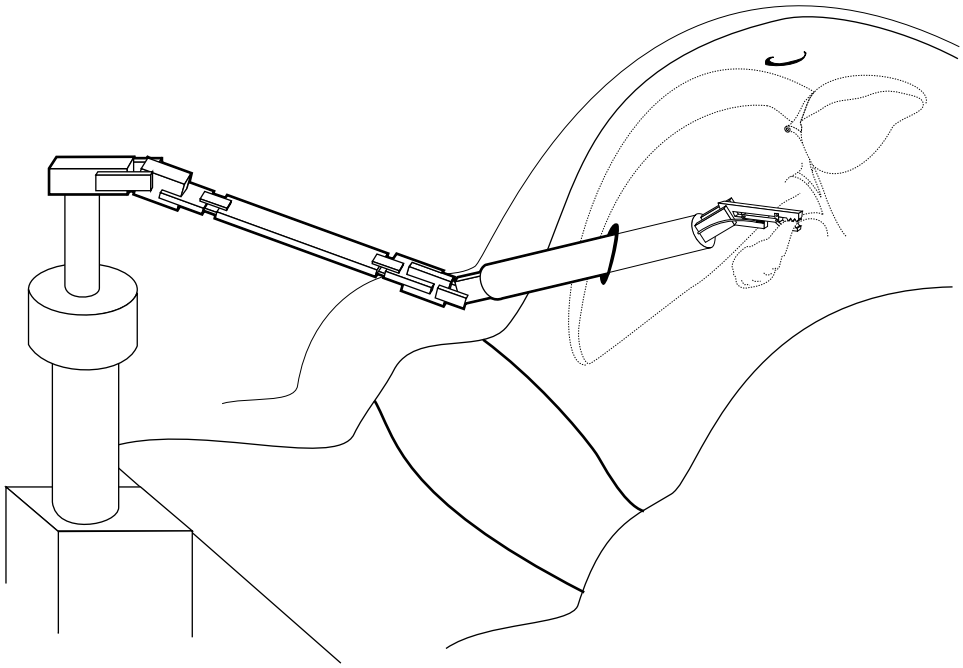

Figure 19: Design of telesurgical workstation slave module.

enough to set up that it will not interfere with operating room procedure or access to the patient in case of an emergency.

References

[1] F. Tendick, R. Jennings, G. Tharp, and L. Stark. Sensing and manipulation problems in endoscopic surgery: Experiment, analysis, and observation. *Presence*, 2(1):66–81, winter 1993.

[2] J. N. Graber, L. S. Schultz, J. J. Pietrafitta, and D. F. Hickok. *Laparoscopic Abdominal Surgery*. McGraw-Hill, San Francisco, 1993.

[3] John Baillie. *Gastrointestinal Endoscopy: Basic Principles and Practice*. Butterworth-Heinemann, Oxford, 1992.

[4] Jerome H. Siegel. *Endoscopic Retrograde Cholangiopancreatography: Technique, Diagnosis, and Therapy*. Raven Press, New York, 1992.

[5] Fred E. Silverstein and Guido N.J. Tytgat. *Atlas of Gastrointestinal Endoscopy*. Gower Medical, New York, 1991.

[6] K. Semm. *Operative Manual for Endoscopic Abdominal Surgery: Operative Pelviscopy, Operative Laparoscopy*. Year Book Medical, Chicago, 1987.

[7] J. W. Saleh. *Laparoscopy*. Saunders, Philadelphia, 1988.

[8] M. Cohn, C. Deno, and J. Fuji. Hydraulic actuator, robot containing same, and method of producing same. U.S. Patent Application, 1993.

[9] J. M. Wendlandt. Milli robotics for endoscopy. ERL technical report UCB/ERL M94/7, University of California at Berkeley, 1994. Department of EECS.

[10] J. M. Wendlandt and S. S. Sastry. Design and control of a simplified stewart platform for endoscopy. In *IEEE 33rd Conference on Decision and Control*, Lake Buena Vista, FL, December 1994.

[11] K. Suzumori, S. Iikura, and H. Tanaka. Development of flexible microactuator and its application to robotic mechanisms. In *IEEE International Conference on Robotics and Automation*, pages 1622–1627, Sacramento, CA, April 1991.

[12] C. Deno, R. Murray, K. Pister, and S. Sastry. Finger-like biomechanical robots. ERL Technical Report, University of California at Berkeley, 1992. Department of EECS.

[13] M. Cohn, M. Lam, and R. S. Fearing. Tactile feedback for teleoperation. In *Telemanipulator Technology, SPIE Proc. 1833*, pages 240–254, Boston, November 1992.

[14] R. S. Fearing. Tactile sensing mechanisms. *International Journal of Robotics Research*, 9(3):3–23, June 1990.

[15] B. Gray. A surface-machined capacitive microtactile sensor. Research in progress, U.C. Berkeley, EECS Department, 1995.

[16] H. P. Schwan. Dielectric properties of cells and tissues. In A. Chiabrera, C. Nicolini, and H. P. Schwan, editors, *Interactions Between Electromagnetic Fields and Cells*. Plenum Press and NATO Scientific Affairs Division, New York, 1985.

[17] E. H. Grant, V. E. R. McLean, N. R. V. Nightingale, and C. Gabriel. Dielectric properties of water in biological solutions. In A. Chiabrera, C. Nicolini, and H. P. Schwan, editors, *Interactions Between Electromagnetic Fields and Cells*. Plenum Press and NATO Scientific Affairs Division, New York, 1985.

[18] K. V. I. S. Kaler and T. B. Jones. Dielectrophoretic spectra of single cells determined by feedback-controlled levitation. *Biophysical Journal*, 57:173–182, February 1990.

[19] T. L. Brooks. Telerobotic response requirement. In *IEEE International Conference on Systems, Man and Cybernetics*, pages 113–120, Los Angeles, Nov. 4-7 1990.

[20] T. L. Brooks and A. K. Bejczy. Hand controllers for teleoperation. JPL Publication 85-11, JPL, March 1985.

[21] G. Burdea and J. C. Zhuang. Dextrous telerobotics with force feedback - an overview: 1. human factors. *Robotica*, 9:171–178, April-June 1991.

[22] P. Fischer, R. Daniel, and K. V. Siva. Specification and design of input devices for teleoperation. In *IEEE Conference on Robotics and Automation*, pages 540–545, Cincinnati, 1990.

[23] D. A. McAffee and P. Fiorini. Hand controller design requirements and performance issues in telerobotics. In *Fifth International Conference on Advanced Robotics*, pages 186–192, Pisa, Italy, 1991.

[24] T. B. Sheridan. *Telerobotics, Automation, and Human Supervisory Control*. MIT Press, Cambridge, MA, 1992.

[25] A. K. Bejczy and K. Salisbury. Controlling remote manipulators through kinesthetic coupling. *Computers in Mechanical Engineering*, 2:48–60, July 1983.

[26] V. Hayward, C. Nemri, X. Chen, and B. Duplat. Kinematic decoupling in mechanisms and application to a passive hand controller design. *Journal of Robotic Systems*, 10(5):767–790, July 1993.

[27] K. V. Siva, A. A. Dumbreck, P. J. Fischer, and E. Abel. Development of a general purpose hand controller for advanced teleoperation. In *International Symposium on Teleoperation and Control*, pages 277–290, Bristol, England, 1988.

[28] H. Eglowstein. Reach out and touch your data. *Byte*, 15(7):283–290, July 1990.

[29] J. Hong and X. Tan. Calibrating a vpl dataglove for teleoperating the utah/mit hand. In *IEEE Conference on Robotics and Automation*, pages 1752–1757, Scottsdale, AZ, 1989.

[30] L. Pao and T. H. Speeter. Transformation of human hand positions for robotic hand control. In *IEEE Conference on Robotics and Automation*, pages 1758–1763, Scottsdale, AZ, 1989.

[31] B. A. Marcus, P. J. Churchill, and A. D. Little. Sensing human hand motions for controlling dexterous robots. In *Lyndon B. Johnson Space Center 2nd Annual Workshop on Space Operations Automation and Robotics (SOAR)*, pages 481–485, 1988.

[32] Virtual Technologies, Palo Alto, CA. *Price list*, 1994.

[33] A. K. Bejczy. Sensors, controls, and man-machine interfaces for advanced teleoperation. *Science*, 208(4450):1327–1335, June 1980.

[34] J. E. E. Sharpe. Technical and human operational requirements for skill transfer in teleoperations. In *International Symposium on Teleoperation and Control*, pages 175–187, Bristol, England, 1988.

[35] J. W. Hill. Study to design and develop remote manipulator systems. NASA contract nas2-8652, NASA-CR-152092, SRI project 4055, JPL, July 1976.

[36] J. W. Hill. Study of modeling and evaluation of remote manipulation tasks with force-feedback. Technical report, JPL contract 95-5170, JPL, March 1979.

[37] R. D. Howe. A force-reflecting teleoperated hand system for the study of tactile sensing in precision manipulation. In *IEEE International Conference on Robotics and Automation*, pages 1321–1326, Nice, France, May 1992.

[38] G. Burdea and J. C. Zhuang. Dextrous telerobotics with force feedback - an overview: 2. control and implementation. *Robotica*, 9:291–298, July-September 1991.

[39] R. M. Anderson and R. F. Romfh. *Technique in the Use of Surgical Tools*. Appleton-Century-Crofts, New York, 1980.

[40] L. S. Crawford. A dextrous master for telesurgery. ERL technical report UCB/ERL M93/95, University of California at Berkeley, 1993. Department of Electrical Engineering and Computer Science.

[41] E. J. Nicolson and R. S. Fearing. Sensing capabilities of linear elastic cylindrical fingers. In *IEEE/RSJ International Conference on Intelligent Robots and Systems*, Yokohama, Japan, July 1993.